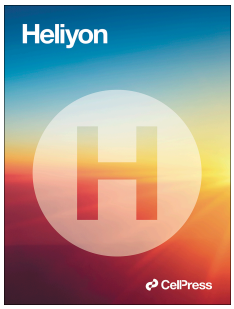

Development and characterization of amphotericin B nanoemulsion-loaded mucoadhesive gel for treatment of vulvovaginal candidiasis

Mrunal U. Patil, Amarjitsing Rajput, Veena S. Belgamwar, Shailesh S. Chalikwar

PII: S2405-8440(22)02777-3

DOI: https://doi.org/10.1016/j.heliyon.2022.e11489

Reference: HLY 11489

To appear in: *HELIYON*

Received Date: 29 July 2022

Revised Date: 22 October 2022

Accepted Date: 3 November 2022

Please cite this article as: M.U. Patil, A. Rajput, V.S. Belgamwar, S.S. Chalikwar, Development and characterization of amphotericin B nanoemulsion-loaded mucoadhesive gel for treatment of vulvovaginal candidiasis, *HELIYON*, https://doi.org/10.1016/j.heliyon.2022.e11489.

DEVELOPMENT AND CHARACTERIZATION OF AMPHOTERICIN B NANOEMULSION-LOADED MUCOADHESIVE GEL FOR TREATMENT OF VULVOVAGINAL CANDIDIASIS

Mrunal U. Patil[1,2#], Amarjitsing Rajput[3#], Veena S. Belgamwar [4*], Shailesh S. Chalikwar[1*]

[1]Department of Pharmaceutics and Quality Assurance, R. C. Patel Institute of Pharmaceutical Education and Research, Shirpur 425405, Maharashtra State, India.

[2]Centre Interdisciplinaire de Nanoscience de Marseille (CINaM), Aix-Marseille-Université (luminy), 163, Avenue luminy,13288 Marseille, France.

[3]Department of Pharmaceutics, Bharti Vidyapeeth Deemed University, Poona College of Pharmacy, Erandwane, Pune 411038, Maharashtra, India.

[4]University Department of Pharmaceutical Sciences Rashtrasant Tukadoji Maharaj, Nagpur University, Nagpur 440033, Maharashtra, India

[*]Corresponding Authors,
Dr. (Mrs.) Veena S. Belgamwar
Professor
University Department of Pharmaceutical Sciences
Rashtrasant Tukadoji Maharaj, Nagpur University
Mahatma Jyotiba Phule Shaikshanik Parisar
Amravati Road, Campus, Nagpur-440033
Maharashtra, India
Telephone No- 0712-2500324
Fax--+91-712-2500355
Email- vbelgamwar@gmail.com

Dr. Shailesh S. Chalikwar
Professor and Head,
Industrial Pharmacy & Quality Assurance Department,
R. C. Patel Institute of Pharmaceutical Education & Research,
Karwand Naka, Shirpur - 425405,
Dist-Dhule, Maharashtra, India.
Tel No.: + 91-2563-255189
Fax No.: + 91-2563-251808
Email: pharmashailesh@rediffmail.com

[#]Both the first authors have contributed equally.
[*]Both the corresponding authors have contributed equally.

Abstract

Despite being recognized as the "gold standard" for treating azole-resistant vulvovaginal candidiasis, amphotericin B (AmB), an amphoteric molecule, has not been widely used due to serious issues with solubility and permeability. In light of the aforementioned, the objective of the present study was to increase AmB's therapeutic efficacy by formulating it into an o/w nanoemulsion (AmB-NE) system. Furthermore, to facilitate AmB-NE's retention within the vaginal cavity, it was loaded into a mixture of Carbopol® 974P and *Aloe vera*-based gel (CA gel). Briefly, in the present study, a kinetically stable batch of formulated AmB-NE having a globule size of 76.52 ± 3.11 nm, PDI of 0.342 ± 0.032, and zeta potential of -22.32 ± 0.88 mV was incorporated into the CA gel base. This AmB-NE loaded gel (AmB-NE gel) exhibited a non-Fickian/anomalous diffusion from the hydrophilic matrix. The texture analysis of AmB-NE gel revealed that the prepared gel was a non-drip, soft, easy to spread, and sufficiently cohesive gel that could reside in the vaginal cavity, which was confirmed by our *ex-vivo* retention test, which revealed that AmB-NE loaded gel could stay in the vaginal cavity for approximately 11 hours. *Ex-vivo* skin permeation studies revealed that AmB-NE is 4.26 times more permeable than AmB-coarse gel, implying that AmB-NE facilitates AmB entry into the vaginal epithelial layers. Furthermore, *in-vivo* vaginal lavage studies revealed that AmB-NE gel permeated 7.03-fold more than AmB-coarse gel. Prepared AmB-NE gel was stable in refrigerated condition and showed no histopathological toxicity. Thus, the present study suggests that AmB-NE gel could eliminate the existing problem of AmB and that it could serve as an alternative option to treat vulvovaginal candidiasis.

Keywords: Amphotericin B; Nanoemulsion; *Aloe vera* gel; Vaginal candidiasis; Vaginal lavage test.

1. Introduction

Candida albicans causes vulvovaginal candidiasis (VVC), often known as vaginal thrush, which is an acute inflammatory mucocutaneous infection of the vulva and vagina (opportunist yeast) [1–3]. VVC is often the reason for gynaecological advice in women [4]. Approximately 75% of women experience VVC during their lives, and about 40-50% suffer from multiple episodes [5]. Furthermore, physicians have discovered that most women suffer from recurrent VVC (RVCC). Failure to initiate a maintenance regimen results in a mycologic and clinical relapse of vaginitis in 50 % of patients within three months [6]. However, around 10-20% of women will have complex cases of VVC, which comprise enduring non-albicans Candida infection, recurring VVC and severe VVC [7]. Unfortunately, VVC and RVCC have been long neglected by different pharmaceutical organizations, public authorities, funding agencies and scientists across the globe [8]. Both VVC and RVVC are typically treated with topical drug formulations, most commonly vaginal creams, pessaries, and suppositories containing imidazole, triazole, or nystatin, administered once a day for up to 14 days. If resistance develops, oral fluconazole or itraconazole may be administrated for 6 months [9]. In 2016, Johal et al discussed that most of these therapies are quite effective. However, they are still associated with several limitations, toxicity, relapses, dermatitis, etc [10]. Azole antifungal agents serve as the first choice of treatment. Nonetheless, they face a common problem of drug-resistant thrush and relapse of candidiasis, especially in people living with HIV (human immune deficiency virus) for many years [11]. Hence, intravenous amphotericin B (AmB) is often used to treat people for whom azole therapy has failed [12–14]. In managing fungal life-threatening fungal infections, amphotericin B, a polyene antifungal antibiotic, has become the "gold standard" [15]. Regrettably, it is well known that long-term administration of AmB has been associated with severe renal toxicity. Therefore, researchers have considered the vaginal route for AmB delivery in RVCC and VCC. Reports suggest that the comparative efficacy of local versus oral treatment of vulvovaginal candidiasis was not significant between either treatment modality [16,17]. Henceforth, topical vaginal administration of AmB can prove to be equipotent to the oral delivery system. However, using AmB in the vaginal cavity may pose a challenge as it exhibits low solubility, low permeability, and considerable toxicity. Since then, several attempts have been made to develop lipid-based nano-systems of AmB to address said issues. One such effort was the development of Ambisome, an AmB liposome formulation that improved AmB's efficacy to eradicate concentrated fungal inoculums without escalating its toxicity [18]. However, the physical and chemical instability of its storage makes liposomal drug delivery challenging for formulation scientists and designers [14,19]. Furthermore, the

high cost of excipients and the requirement for lyophilisation have prompted many to consider much more cost-efficient lipid-based nanosystems for formulating AmB. Nanoemulsion (NE) consist of very small emulsion droplets, with sizes less than ~300 nm. It is stabilized by a strong interfacial film of surfactant and cosurfactant/cosolvent molecules. The kinetics of destabilization of nanoemulsions is so slow (~months) hence, they are considered to be kinetically stable [20]. Higher solubilising capacity of lipophilic molecules, large surface area and the low interfacial tension of o/w nanoemulsion allows an efficient penetration of lipophilic active agent. In 2015, Mutlaq et al. found that incorporating an amphoteric acyclovir into NE increased its solubility and caused a two-fold increase in its skin permeation when compared to the marketed gel [21]. Similar findings were made for a miconazole nitrate nanoemulsion, where the researchers discovered that encapsulating the miconazole nitrate within the oil globules of Peceol (oil phase) resulted in decreased haemolysis and toxicity, as well as improved permeability and solubility [22]. Drawing spur from the aforementioned research articles, authors of the current investigation have developed an oil-in-water (o/w) nanoemulsion loaded with AmB (AmB-NE) to tackle difficulties associated with conventional AmB therapy. However, the efficacy of AmB-NE may be limited by its residence time in the genitourinary tract due to the self-cleaning action of the vaginal tract system [23]. Therefore, in order to achieve residence at the targeted site for a relatively long period, decrease fluctuations in the drug dose level, and decrease dosing frequency, a semi-solid formulation consisting of nanoemulsion was developed. Although widely marketed semi-solid preparations for vaginal drug delivery include creams, ointments, and suppositories, the demerits associated with them (e.g., messiness, discomfort, washing or by natural factors, and leakage) make them non-patient compliant. As a result, in the current study, AmB-NE was loaded into a three-dimensional, polymeric mucoadhesive gel matrix because gels are reported to be better tolerated in the vaginal area than any other dosage form, thus making them more patient acceptable [24]. Simple mucoadhesive gels frequently dry out the vaginal cavity, exacerbating candidiasis symptoms. In such circumstances, an effective humectant is required. As a result, the author decided to include *Aloe vera* leaf gel, a natural humectant, in the current formulation [25]. *Aloe vera* leaf gel has excellent antimicrobial, antifungal [26], and anti-inflammatory activity [27]. Numerous studies have found that *Aloe vera* gel has good penetrating and hydrating effects on the skin's layers in addition to being an excellent emollient and emulsifier [28–30].

2. Materials and Methods

2.1 Materials

Amphotericin B was obtained as a gift from Bharat Serum and Vaccines Ltd., Thane, India; Capmul MCM (glyceryl mono-dicaprylate) was supplied by Abitech Corporation through Indchem International, Mumbai, India; Cremophore RH 40 (PEG 35 castor oil) was obtained from BASF India Ltd., Mumbai, India; and Transcutol HP (Highly purified diethylene glycol monoethyl ether) was obtained from Gattefosse, Lyon, France. The gelling agent, Carbopol® 974P, was a kind gift from Noveon, Inc. Cleveland, OH, USA. Aloe vera gel was purchased from D. Jain's Eco-friendly Industries, India. All other reagents used were of analytical grade.

2.2 Screening of oils, surfactants and co-surfactants

2.2.1 Screening of oils

The solubility of AmB's in various oils was evaluated by dissolving an extra amount of the drug in 5 mL of oils alone or in combination (Peceol, Capmul MCM, Capmul PG8, oleic acid, Labrafac, castor oil, isopropyl myristate (IPM), Peceol + castor oil, Peceol + Capmul MCM, Capmul MCM + castor oil) in stopper vials of 30 mL and mixed by a vortex mixer. The mixtures in the vials were allowed to reach equilibrium at 25 ± 1.0 °C for 48 h in an isothermal shaker [Nirmal International, India]. After equilibration, the samples were withdrawn and centrifuged for 15 min at 3000 rpm. The supernatant was filtered using a 0.45 µ membrane filter, and the concentrations of the AmB in oils were determined by High-Performance Liquid Chromatography (HPLC) [Agilent 1200, USA][31].

2.2.2 Screening of surfactants

A vortex mixer was used to vigorously mix each of the screened oils with 1 mL of surfactant solution (20% w/w). The oil was gradually added until the solution became hazy; in some cases, the uniform, clear solution could be seen. The total amount of oil added was recorded [32].

2.2.3 Screening of co-surfactants

Co-surfactants are essential for lowering interfacial tension, enhancing interface fluidity, and increasing the mobility of the hydrocarbon tail [33]. To formulate a nanoemulsion, a co-surfactant should be selected to reduce the total surfactant concentration [34]. A mixture of 4 g of screened surfactant and 10 g of screened oil phase was mixed and later diluted by adding 20 mL of distilled water. The resulting mixture (1 mL) was titrated with each co-surfactant (ethanol, Transcutol P, propylene glycol and, ethylene glycol) until it turned clear. Later, more

cosurfactants were added until the clear solution became cloudy again, and the total amount of co-surfactant used was noted [32].

2.3 Construction of pseudo ternary phase diagram (selection of S_{mix} ratio)

The pseudo ternary phase diagram studied the impact of surfactant to the co-surfactant ratio (S_{mix}) on the emulsion forming region. One important point should be considered: constructing a pseudo ternary phase diagram only optimizes the S_{mix} ratio and does not generate a formula for nanoemulsion. Based on solubility studies, Capmul MCM, Cremophor RH 40, and Transcutol P were chosen as oil, surfactant, and co-surfactant, respectively. The surfactant and co-surfactant were used in different weight ratios (1:1, 2:1, 3:1, 1:2 and 1:3).

In various glass vials, the drug-dissolved oil phase was mixed with a S_{mix} of varying weight ratios from 1:9 to 9:1 for each phase diagram. Several blends of oil and S_{mix} (1:9, 2:8, 3:7, 4:6, 5:5, 6:4, 7:3, 8:2, and 9:1) were used so that the boundaries of the phases could be identified clearly in the phase diagrams. Chemix software trial version 3.51 was used to plot the pseudo ternary phase diagrams. The aqueous phase was then added slowly to each combination of oil and S_{mix}. The transparency and viscosity of the o/w nanoemulsions were observed [31].

2.4 Selection of formulation batches

a. The objective of drawing a phase diagram was to optimize the S_{mix} ratio. Out of five pseudo-ternary graphs plotted for the various S_{mix} ratios (1:1, 2:1, 3:1, 1:2, 1:3), the S_{mix} with the highest nanoemulsion region in the phase diagram was selected.

b. Considering the solubility of the AmB (1.67 mg/mL of oil), a minimum of 6 mL of oil was needed to solubilize the dose of 10 mg of AmB (24% of 25 mL).

c. Various ratios of oil and optimized S_{mix} (SOR) were used to produce nanoemulsion. The effect of increasing oil proportion when surfactant was kept constant and the impact of increasing surfactant proportion when oil was kept constant were studied.

d. The formulations were checked for drug precipitation and stored for 24 h at room temperature.

e. The formulation containing less surfactant and co-surfactant was chosen to formulate nanoemulsion.

2.4.1 Optimization of formulation

Over the past many years, microemulsions have been confused with nanoemulsions. Stress testing (dilution and temperature testing) was performed to decisively determine the nature of

the formulation system. The variation in temperature and dilution significantly impacts the nanostructures of microemulsions, which can even break them up, whereas nanoemulsion droplets stay stable. Nanoemulsions contain tiny globule sizes, which prevent the droplets from flocculating and coalescing [20,35]. As a result, the following experiments were performed to optimize the formulation.

2.4.1.1 Dilution testing

To test the influence of dilution on globule size, each formulation batch was diluted 10 to 100 times in a continuous phase. The mean globule size and PDI was recorded at an angle of 90° by using a zetasizer instrument (Malvern Instruments, UK) operated at 25 °C. The experiments were performed in triplicate [36].

2.4.1.2 Testing at a higher temperature

Each formulation batch was stored at 45 °C for 48 h. The effect of the increased temperature on the mean globule was observed. The experiment was carried out in triplicate [36].

2.4.1.3 Ostwald ripening

Those formulation batches that exhibited no noticeable change in mean globule size on dilution nor elevated temperature were subjected to the Ostwald ripening test for 90 days. A plot of the cube of the globule's radius (r^3) versus time (t) was used to quantify Ostwald ripening. Hence, the globule diameters of those formulation batches that passed the stress test were evaluated as a function of time, and the rate of Ostwald ripening was determined as the slope of the plots. The formulation with the lowest rate of Ostwald ripening was chosen for inclusion in the gel basis (AmB-NE). The study was conducted in triplicate [36].

2.5 Formulation of **AmB-***loaded nanoemulsion (AmB-NE)*

A weighed amount of AmB (10 mg) was dissolved in Capmul MCM (24% w/w). The resulting oil phase was thoroughly mixed for 24 h using a stirrer. On a subsequent day, 36% w/w S_{mix} (2:1) was added to the oil phase and vortexed for 10 min in a 30 mL screw-capped bottle. The double distilled water was then gradually added to the mixture while being vortexed to create a nanoemulsion.

2.6 Characterization of AmB-NE

2.6.1 Globule diameter analysis, polydispersity index and zeta potential

Using a zetasizer, the mean globule diameter and polydispersity index of the AmB-NE were evaluated using a particle size analyzer [Malvern Instruments, UK]. The AmB-NE was suitably diluted with deionized water. The surface charge of the AmB-NE was calculated using the Smoluchowski equation post determining the zeta potential using the same instrument. Zeta potential measurements were performed at a temperature of 25 °C and electric field strength of 23 V/m. The globule diameter, polydispersity index and zeta potential values were obtained as the averages of three measurements [37–39].

2.6.2 Effect of S_{mix} and oil ratio on mean globule diameter of AmB-NE

The influence of different concentrations of S_{mix} (24-90% w/w) and oil (24-48% w/w) on the mean globule diameter of the AmB-NE nanoemulsion was studied. Studies were conducted using a zetasizer instrument operated at 25 °C. These experiments were carried out in triplicate using a zetasizer.

2.6.3 Viscosity, pH and visual appearance of AmB-NE

The viscosity of the AmB-NE (F7) was measured using Brookfield Rheometer equipped with a spindle 00 UL adaptor [Brookfield Engineering Labs., Inc., USA], and the pH of the nanoemulsion was determined using a pH meter [Systronics Ltd., India] at 25 °C. The average of three data points was obtained. Nanoemulsions with low mean globule size may look transparent, and the slightest evidence of destabilization can be easily recognized by holding the nanoemulsion against a readable background. In such case, the transparency of the nanoemulsion should not change before and after drug loading [40].

2.6.4 Conductivity study

A conductivity study was used to determine the class of nanoemulsion, oil-in-water (o/w) or water-in-oil (w/o). The nanoemulsion (F7) conductivity was tested by a conductivity meter [Systronics Ltd., India]. The study was conducted at 25 ± 1 °C in triplicate. If the formulation is of the o/w type, it is anticipated that a current will pass through the continuous phase, i.e., water, causing a deflection. No deflection indicates that the continuous phase is oil, implying that the emulsion system is w/o [41].

2.6.5 HPLC analysis of AmB in AmB-NE

The amount of AmB in the F7 batch was measured using HPLC immediately after preparation. Briefly, 5 mL of nanoemulsion was dissolved in 10 mL of methanol and then centrifuged [Remi Instruments, India] at 3500 rpm for 15 min. The drug content was quantified using an HPLC system [Agilent 1200, USA] with a UV detector comprised of a quaternary pump and a diode array detector [42,43]. The drug was eluted on a reverse-phase C18 column (4.6 mm×150 mm, internal diameter 5 µm, Eclipsed XDB, Singapore) using a mobile phase consisting of Acetonitrile: Acetic acid (10%): Water (41:43:16) flowing at the rate of 1.0 mL/min. The results were recorded at 407 nm at 25 °C. The retention time was determined to be 3.4 minutes [44].

2.6.6 *In-vitro* drug release study

A modified method of *in-vitro* release of AmB from AmB-NE was performed by placing nanoemulsion (F7) equivalent to 1 mg of AmB in a dialysis bag (MWCO-12,000 g/mole; Sigma, USA) that was previously activated by being soaked overnight in citro-phosphate buffer (pH 4.5). This AmB-NE loaded dialysis bag was fixed to a static shaft and dipped in 50 mL of citro-phosphate buffer containing 1 mL of dimethyl sulphoxide (DMSO): methanol (1:1) at 37 ± 0.5 °C and stirred at 100 rpm. At definite time intervals of 0, 20, 40, 60, 80, 100, and 120 min, 1 mL sample was removed and replaced with buffer to preserve the sink condition. The samples were examined to determine the drug concentration by HPLC at 407 nm in triplicate [45,46]

2.6.7 Stability of AmB-NE

2.6.7.1 Chemical stability of AmB

The F7 batch of the nanoemulsion was formulated and preserved at 5 ± 3 °C and 25 ± 2 °C, 60 ± 5% RH for 6 months. At 0, 60, 120 and 180 days, samples were removed and studied for drug content (remaining) by HPLC at 407 nm. Finally, the graph of the percentage of drug remaining against time was plotted [47]. The experiment was performed in triplicates.

2.6.7.2 Chemical stability of AmB-NE

Chemical deterioration of the oil components and surfactants may occur as a result of hydrolysis or oxidation. This also causes a decrease in the pH level [48]. The pH of different nanoemulsion batches was determined at the prescribed period (0, 60, 120 and 180 days) over 6 months. The formulation was investigated in triplicate (at 5 ± 3 °C and 25 ± 2 °C, 60 ± 5 % RH) using a pH meter [Systronics, Ltd, India][49].

2.6.7.3. Physical stability of AmB-NE

The F7 batch of the nanoemulsion stored at 5 ± 3 °C and 25 ± 2 °C, 60 ± 5% RH was observed for physical changes viz. mean globule, zeta potential, and PDI. Changes in viscosity were also noted as a secondary factor of stability [47,50].

2.7 Preparation of AmB-NE loaded gel

Carbopol®974P (1% w/w) was dissolved in distilled water, and a sufficient amount of triethanolamine was added to achieve pH 4.5 ± 0.1. The resulting gel formation was kept at 2-8 °C for 24 h to remove entrapped air. The following day, *Aloe vera* gel was added to prepared Carbopol® 974P gel in 1:1 w/w. Finally, the final screened batch of nanoemulsion (15 mL) was slowly added to 3 g of CA gel base using a stirrer [51–54].

2.8 Characterization of AmB-NE loaded gel

2.8.1 Determination of total drug content in AmB-NE gel

In a 100 mL volumetric flask, 1 g of AmB-NE gel was weighed and dissolved in a 2 % DMSO: methanol solution (1:1). This was diluted appropriately with methanol and analyzed using the previous HPLC analysis [50]. This experiment was carried out in triplicate, and the total drug content was calculated using Equation 1.

$$\text{Total drug content} = \text{estimated drug content} \times \text{total quantity of of gel} \qquad \text{Eq. (1)}$$

2.8.2 Rheological behaviour, spreadability, penetrometry and texture profile analysis (TPA) of AmB-NE-loaded gel

The viscosity of the CA gel and the AmB-NE-loaded gel was measured using spindle no.7 [Brookfield Engineering Labs. Inc., DV-E, USA]. The apparent viscosity was measured at 25 °C with spindle speeds of 5, 10, 30, 50, 60 and 100 rpm [54]. The Brookfield texture analyzer [Brookfield Engineering Laboratories, Inc, CT3, USA] was operated in TPA mode to measure sensory properties of gel such as consistency, stiffness, cohesiveness, and work of adhesion. The probe was programmed to descend into the sample at 0.5 mm/s to a depth of 30 mm, then return to its original position at the same pace. The maximum force required for separating from the gel was measured. During testing, special precautions were taken to ensure that the probe did not touch (or even come close to) the container's walls or base, as this could result in erroneous results. Similarly, the gel's spreadability and penetrometry were determined using the

same instrument with a 40º cone probe (clear acrylic, 29 mm diameter, 41 mm length) operated in compression mode. These experiments were carried out in triplicate [55].

2.8.3 *Ex-vivo* mucoadhesive test

2.8.3.1 Preparation of vaginal mucosa

The mucoadhesive strength of the AmB-NE loaded gel was assessed using bovine vaginal mucosa. Fresh vaginal mucosal tissue was obtained from a local abattoir. The mucosa was cleaned, washed with isotonic saline, and stored at -20 °C. Before the experiment, the vaginal mucosa was treated with 0.1% sodium azide, longitudinally sliced, and allowed to reach room temperature.

2.8.3.2 Procedure

A Brookfield CT3 Texture analyzer [Brookfield Engineering Laboratories, Inc, USA] was used to evaluate the mucoadhesive strength of the AmB-NE gel. The experiment was performed as per the technique developed by Neves et al [16]. Vaginal mucosa was subjected to a regular saline bath (37 °C, 60 min) for defrost, cleaned and tied to the instrument probe (cylindrical, 25 mm diameter) before the mucoadhesive measurements. The mucosal surface that covered the probe's bottom end was meticulously examined to ensure it was flat. After that, mucosal tissue was submerged in a simulated vaginal fluid for 15 min at 37 °C. Evaluation was conducted using set parameters (preload: 1 N, contact time: 3.0 min, diameter of upper probe: 36 mm, pretest speed: 0.5 mm/s, and test speed: 0.1 mm/s). The probe was then lowered at a controlled rate until it came into contact with the gel surface. The probe's constant downward pull on the sample surface ensured close contact between the mucosa and gel. After a predetermined time (mucosal contact time) and a normal speed (probe speed), the probe was brought to its original location above the AmB-NE gel. In conclusion, the force and work done were measured. This study was conducted in triplicate.

2.8.4 *Ex-vivo* retention measurement

A piece of bovine vaginal mucosa was trimmed to the desired size and angled at 45º to the horizontal plane polyethylene plate. The thread ends of the vaginal mucosal tube were then attached to the top and lower ends of the plate using thread. Using an applicator, 1 g of AmB-NE gel was injected into the vaginal cavity. A 5 min preload time was given when the formulation was placed in the vaginal tube to ensure it adhered to the vaginal walls. Peristaltically pumped phosphate buffer (pH 4.5) warmed to 37 ± 0.5 °C over the vertically

suspended vaginal tube containing the formulation at a 3 mL/min rate. The formulation was discharged from the lower end of the cell, which was recorded [56,57]. The experiment was performed in triplicates.

2.8.5 *In-vitro* drug release study from gel

Using a modified USP XXIII apparatus I at 37 ± 0.5 °C, the *in-vitro* release patterns of AmB-NE gel and coarse AmB gels were examined. A stainless-steel wire screen (350 µm mesh size sinker) was used to tightly fasten a watch dish containing 10 mg AmB-equivalent formulated compound. The dish was then immersed in 500 mL of citro-phosphate buffer (pH 4.5) containing 2% DMSO and methanol (1:1) in a USP dissolution test apparatus. The spindle speed was set at 25 rpm. During the investigation, 2 mL aliquots of the dissolution medium were taken at predefined time intervals (0.5, 1, 1.5, 2, 4, and so on up to 12 h) and replaced with fresh media. A 0.45 µ nylon membrane filter was utilized to filter the samples, and the amount of AmB released was measured using the HPLC [55].

The experiment was performed in triplicates. To evaluate the release mechanism of AmB-NE gel, the results were fitted into Korsmeyer-Peppas equation, as shown in Equation 2.

$$\text{Log } Mt/M\infty = \log K + n \log t \qquad \text{Eq. (2)}$$

Where M_t is the concentration of drug released at time t,

M_∞ is total drug content,

k is constant for the geometrical and structural property of the device

n is drug release mechanism exponent

2.8.6 *Ex-vivo* skin permeation studies

2.8.6.1 Experimental set-up for permeation study

Ex-vivo skin permeation tests using bovine vaginal mucosa were performed on an amber-colour Franz diffusion cell (diffusion area of 3.14 cm^2, capacity of 15 mL). Before the experiment, frozen specimens were thawed in citro-phosphate buffer (pH 4.5) for 10 min. The thawed vaginal mucosal specimens were carefully cut without damaging the epithelial surfaces. The mucosal sections were then mounted onto diffusion cells. The receiver compartment was filled with citro-phosphate buffer (pH 4.5), with 2% DMSO and methanol (1:1) used as the diffusion medium. The donor compartment was filled with one gram of AmB-NE gel, and to achieve

occlusive conditions, the compartments were sealed with paraffin film. At regular intervals (0, 2, 4, 6, 24 h), 1 mL aliquots were collected, filtered through a 0.45µ membrane filter, and evaluated by HPLC. The experiment was performed in triplicates.

2.8.6.2 Permeation data analysis

The total amount of drug penetrating through the skin (g/cm^2) was plotted against time (min). The two crucial permeation study parameters, i.e., drug flux (permeation rate) at steady state (J_{ss}), were determined by dividing the slope by the area of the Franz diffusion cell.

Using Eq. 3, the permeability coefficient (K_p) was obtained by dividing the steady state drug flux by the total concentration of drug used in the experiment (C_o).

$$K_p = J_{ss}/C_o \qquad \text{Eq. (3)}$$

The enhancement ratio (E_r) was calculated using Eq. 4.

$$E_r = (J_{ss} \text{ of AmB-NE gel}) / (J_{ss} \text{ of coarse AmB gel}) \qquad \text{Eq. (4)}$$

2.8.7 Stability study of AmB-NE gel

The stability of the AmB-NE loaded gel was assessed at 5 ± 3 °C for 6 months. The AmB-NE loaded gel was wrapped in 5 g aluminium ointment tubes. Samples (n=3) were withdrawn at 0, 60, 120 and 180 days and were analyzed for pH and content using HPLC [55].

2.8.8 *In-vitro* antifungal activity

The cup plate method was used to conduct antimicrobial studies on *Candida albicans* (MTCC 183 strain). Briefly, 25 mL of sterilized Sabouraud dextrose agar was placed in sterilized 15 cm diameter Petri plates and allowed to solidify in laminar airflow. The Candida albicans concentration in the inoculum was equivalent to $5x10^{15}$ CFU/mL. On solidified Sabouraud dextrose agar, an aqueous suspension of *Candida albicans* was evenly dispersed. The cups were aseptically cut and filled with DMSO solubilized AmB (20 µg/mL), AmB-NE (20 µg/mL), AmB-NE gel (250 mg containing 20 µg/mL AmB), and *Aloe vera* gel base (250 mg) using sterile syringes. The plates were covered with lids and incubated for 40 h at 32 ± 5 °C [55,56,58].

2.9 In-vivo vaginal lavage testing

Instead of using an infection model that involves inoculating *Candida albicans* inside rat's vaginal cavities followed by examining microbial growth suppression using test therapy, a simple method was used in this study to study the efficacy of AmB-NE gel. A modified protocol approved by CPCSEA and the local animal ethical committee (Regd. No. 651/PO/ReBi/S/02/CPCSEA) was used. Ten female Sprague Dawley rats were housed in an animal house with a temperature of 25 °C, relative humidity of 45-55%, and a 12 h dark-light cycle. They were fed and watered *ad libitum*. All selected rats were kept in a pseudoestrous phase by subcutaneous administration of estradiol benzoate (25 mg/kg). Two groups were made, containing five animals each. A dose of 2 mg/kg of AmB-NE gel was applied in the vaginal cavities of the rats of the first group, and the second group received 2 mg/kg of coarse-AmB dispersed in the gel. After 24 h, vaginal lavage samples were collected by cleaning the vagina three times with saline. The volume of vaginal lavage collected from each rat was diluted with an appropriate solvent, filtered to eliminate any cell debris and analyzed for AmB content using HPLC. The amount of AmB permeated through the vaginal epithelium was assessed by subtracting the content obtained in the lavage from the total content applied [59,60]

2.10 Histological study

A histological examination of the vaginal tissue was carried out to ensure that the formulation and its contents are safe and do not cause any damage to the vaginal epithelium. The study was approved by CPCSEA and the local animal ethical committee under registration number 651/PO/ReBi/S/02/CPCSEA. Female Sprague Dawley rats weighing 200 ± 10 g were grouped into five. Each group consisted of five animals each of which received five different treatments namely saline (untreated, blank), AmB-NE, isopropyl alcohol (IPA), CA gel and AmB-NE gel for 24 h. The vaginal tissues were then isolated and preserved in 10% neutral carbonated buffered formaldehyde. For microscopy, these tissues were then embedded in paraffin, and sliced into sections. The slices were then stained with hematoxylin and eosin and analyzed using a Motic microscope (Motic Instruments Inc., China) with a 1/399 CCD camera imaging attachment and computer-controlled image processing software (Motic images 2000, 1.3 version, China).

2.11 Statistical analysis

Graphs were plotted using GraphPad Prism 6 (GraphPad Inc., San Diego, CA). Statistical analysis was performed using either student t-test or one-way ANOVA analysis of variance,

followed by post-hoc Bonferroni multiple comparison tests with a significance level of $p < 0.05$, CI of 95%.

3. Results and discussion

Nanoemulsions improve the drug's solubility and penetration. As a result, this system is best suited to molecules with low solubility and permeability, i.e., BCS class IV.

3.1 Screening of components (oils, surfactants, co-surfactants)

Lipophilic compounds are preferably solubilized in o/w nanoemulsion. It is indeed necessary for the context of nanoemulsions for a drug to be in a completely solubilized form. As a result, the solubility of a drug in an oil phase is critical for oil selection. Drug solubility in surfactants, on the other hand, is unimportant. Because surfactants are responsible for emulsifying and stabilizing the oil droplets, taking drug solubility into account for drug loading within a nanoemulsion system may result in drug precipitation. As a result, it is critical to choose a surfactant based on its capacity to miscibilise oil droplets [61].

In the present investigation, Peceol (1.96 mg/mL) and Capmul MCM (1.67 mg/mL) imparted the highest solubility (**Fig. 1a**). AmB, being highly lipophilic, cannot be solubilized to a greater extent than this, and initially, both the oils were considered for screening the surfactant.

The HLB value is another crucial factor to consider when choosing a surfactant. The clarity and stability of a nanoemulsion depend on the solubilization of the oil in the surfactant. When used topically, an excessive quantity of surfactant might cause skin irritation. Hence, the minimum concentration of surfactant is used in the formulation. Hydrophilic surfactants and cosurfactants are considered to reduce the interfacial energy necessary to form nanoemulsions and thus improve stability. A stable nanoemulsion is developed by taking low and high HLB surfactants in the proper proportions. Several surfactants such as Cremophor RH 40, Cremophor EL, Tween 80, PEG 400, Labrafil and Poloxamer 188 were used to study the selected oil's solubility (Capmul MCM and Peceol). It was noted that, although AmB is well soluble in Peceol, peceol's combination with tested surfactants resulted in an unstable emulsion system. This suggested that Peceol was not miscible with the tested surfactants. In contrast, Capmul MCM miscibilisized in Cremophor RH 40 and Cremophor EL (**Fig. 1b**). When Cremophor EL was diluted with water, it formed a transparent and homogenous nanoemulsion with Capmul MCM, but its flowability was poor. Hence, Cremophor RH 40 was chosen as the surfactant.

While screening the co-surfactants, it was seen that large amounts of Transcutol P could be imbibed within the oil and surfactant mixture, demonstrating that Transcutol P was compatible

with Cremophor RH 40 and Capmul MCM. Nevertheless, Transcutol P is an excellent permeation enhancer agent and is most suitable for topical formulations.

3.2 Pseudoternary phase diagram study

The phase behaviour of the water: Capmul MCM: Cremophore RH 40 + Transcutol P systems at 25 °C are represented in **supplementary Fig. S1**. The phase behaviour of this system was determined only to select the S_{mix} ratio. The highest amount of oil that a particular Smix ratio may solubilize was noted from the phase diagram. A S_{mix} ratio of about 42% w/w (1:1) (**supplementary Fig. S1a**) could solubilize 12% w/w oil. The surface area of the nanoemulsion enhanced as the amount of surfactant enhanced from a S_{mix} ratio of 1:1 to 2:1. (i.e., 24% w/w of (2:1) S_{mix} ratio (**supplementary Fig. S1b**) could solubilize 24% w/w oil possibly as a result of a reduction in interfacial tension, which enhanced the fluidity of the interface and thus the system's entropy. The oil phase may penetrate more deeply into the hydrophobic area of the surfactant monomers [62]. When a S_{mix} ratio of 3:1 (**supplementary Fig. S1c**) was compared to a S_{mix} ratio of 2:1, the nanoemulsion area was found to be slightly lower, which could be owing to the increased surfactant concentration, albeit the greatest quantity of the oil that this ratio of S_{mix} could solubilize was 24% w/w. The region of nanoemulsion in S_{mix} ratios of 1:2 (**supplementary Fig. S1d**) and 1:3 (**supplementary Fig. S1e**) was very small compared with that of 1:1, and the oil was solubilized to a lesser extent. Hence the S_{mix} ratio of 2:1 was optimized for nanoemulsion formulation. The extent to which the surfactant reduces the surface tension of the oil-water interface and the change in dispersion entropy can influence nanoemulsion production. The surfactant level was therefore kept as low as 42% w/w of the total emulsion since a high percentage of surfactant content is known to induce irritation to human skin upon contact.

3.3 Selection of nanoemulsion and stress testing

A series of formulations were studied using a S_{mix} ratio of 2:1 with a minimum of 24% w/w of oil and a maximum of 42% w/w of S_{mix}. The effect of the oil-surfactant ratio was studied carefully, and selected batches (**Table 1a**) were subjected to the stress test. Apart from the batches that passed the stress test (i.e., F7, F10, F11), other formulations showed a decrease in mean globule size on dilution with the continuous phase and increasing temperature, indicating a substantial effect on the emulsion structure and size. Hence, though the failed batches exhibited a nanosize in the true sense, they could be referred to as nano-structured

microemulsions [20]. Thus, the stress test concluded that formulation batches F7, F10, and F11 were nanoemulsions.

All the formulations that passed the stress test were then evaluated for the rate of Ostwald ripening, which showed (**Table 1b**) that F7 had the lowest rate of Ostwald ripening (**Supplementary Fig. S2**). Also, the surfactant concentration in F7 was the least, which was the essential selection criterion for the nanoemulsions. Hence, formulation F7 was suitable for incorporating into the gel base.

3.4 Characterization of AmB-loaded nanoemulsion

3.4.1 Globule size analysis, polydispersity index and zeta potential

The mean globule size, polydispersity index (**Fig. 2a)**, and zeta potential (**Fig. 2b)** of F7 were found to be 76.52 ± 3.11 nm, 0.342 ± 0.032 and -22.32 ± 0.88 m/V, respectively (**Table 1b).**

3.4.2 Effect of S_{mix} and oil ratio on mean globule size of AmB-NE

For a constant amount of oil phase (24% w/w of oil), lower concentrations of S_{mix} (<42% w/w) produced an NE system having a significantly high ($p<0.05$) mean globule size (80-114 nm) as compared with those NE obtained using 42-60% w/w S_{mix} concentration (70-78 nm). It was observed that, at 42-60% w/w S_{mix} concentration, the globule size remained more or less the same (**Fig. 3a**). It was only after 60% w/w of S_{mix}, a significant increase in globule size ($p<0.05$) was observed. This could be explained by the fact that initially increasing concentration of surfactant causes complete coating of oil globule with surfactant layer causing its condensation within tiny droplets until the interfacial tension is reduced enough to stabilise the droplets. This can also be noticed in **Table 1a**, wherein at a constant amount of oil phase (24% w/w), the mean globule size of batch F1 containing 24% w/w of S_{mix} had a larger globule size (114.98 ± 2.8 nm) as compared to that of F10 (71.60 ± 4.6 nm) containing 42% w/w of $S_{mix.}$ It is anticipated that after the stabilization of oil droplets a surplus amount of surfactant causes the formation of multilayer o/w nanoemulsions thereby causing a rise in the globule size [32].

Interestingly, when the S_{mix} content of 36% w/w was kept constant (**Fig. 3b**), an increase in the oil concentration (Capmul MCM) from 24% w/w to 48% w/w resulted in a significant ($p<0.01$) increase in globule size. This behaviour could be anticipated due to the thinning of the surfactant coating over the oil globules as the oil ratio increases thereby causing destabilization of the system and further leading to agglomeration.

3.4.3 Viscosity, pH and visual appearance of AmB-NE

The viscosity of the optimized formulation (F7) was found to be 86.22 ± 1.41 cp. The pH of F7 was 6.83 ± 0.47, which is compatible with vaginal pH values. It was observed that a nanoemulsion without the drug (**supplementary Fig. S3a**) and AmB-NE (**Supplementary Fig. S3b**) were equally clear and sufficiently transparent to visualize the readable background. The AmB loading did not alter the nanoemulsion's transparency and clarity, suggesting complete solubilization of AmB in oil droplets. The foremost difference was that the drug gave AmB-NE a yellow tint. Additional tests suggesting transparency of NE are discussed in supplementary **section S3**.

3.4.4 Conductivity study

The percentage of water has a direct relationship with electrical conductivity. The higher the electrical conductivity, the more water there is in the system, allowing ions to travel freely. The conductivity (σ) of F7 was 493.533 ± 2.187 μS/cm. This indicated the o/w type of formulation.

3.4.5 HPLC analysis of AmB in nanoemulsion

The optimized batch (F7) drug content was found to be 97.98 ± 2.16 %.

3.4.6 *In-vitro* drug release from AmB-NE

According to **(Fig. 4a),** 93.67 ± 4.35% of AmB was released from AmB-NE within the first 2 hours. However, coarse-AmB (data not shown) did not permeabilize across the dialysis membrane and so could not provide a consistent release profile. The solubilization of AmB into nano-sized emulsion droplets may thus be responsible for the AmB release profile observed in AmB-NE.

3.4.7 Stability of nanoemulsion

3.4.7.1 Chemical stability of AmB

After 180 days, it was found that at %AmB content declined significantly ($p<0.01$) at storage condition of 25 ± 2 °C, 60 ± 5% than that of 5 ± 3 °C **(Table 2).** Thus, recommending AmB-NE's storage in refrigerated condition. **Supplementary Fig. S4** shows the percentage of AmB remaining in AmB-NE as a function of storage time at mentioned storage conditions.

3.4.7.2 Chemical stability of AmB-NE

pH change was not noticed in AmB-NE when stored at 25 ± 2 °C, 60 ± 5%. However, AmB-NE stored at 5 ± 3 °C exhibited an increase ($p<0.05$) in pH on day 180 as compared to day 0 (**Table 2**). Though the cause of this shift is unknown, it could be due to chemical changes in the NE components. As a result, it is crucial to keep track of pH changes after AmB-NE is incorporated into a gel system.

3.4.7.3 ~~Kinetic~~ Physical stability of AmB-NE

At 0, 60, 120, and 180 days, the mean globule size, polydispersity index, zeta potential, viscosity, and refractive index were measured. These values increased somewhat with time at 5 ± 3 °C, as shown in **Table 2**, but the changes were not substantial. However, in the case of AmB-NE stored at 25 ± 2 °C, 60 ± 5% RH, there was a considerable increase in the globule size ($p> 0.05$).

3.5 Characterization of AmB-NE-loaded gel

3.5.1 Determination of pH and total drug content

Normal vaginal pH ranges from 3.8 to 5.0. The pH of the AmB-NE loaded gel was 4.72 ± 0.32, implying that it was tolerable in the vaginal cavity. The AmB-NE gel's total AmB content was determined to be 99.60 ± 0.82 %.

3.5.2 Rheological behaviour, spreadability, penetrometry and texture profile analysis (TPA) of AmB-NE-loaded gel

The purpose of studying the rheology of the CA and AmB-NE loaded gel was to check the behavioural change in the gel base's viscosity after adding the nanoemulsion to the gel base. It was observed from multipoint viscosity measurements that the CA gel's viscosity was reduced significantly on dilution with nanoemulsions. Also, both the CA and AmB-NE loaded gel demonstrated pseudo-plastic behaviour (data not shown).

Texture profile analysis (TPA) was used to determine the mechanical (sensory) properties of the AmB-NE gel. The output of the TPA analysis, penetrometry and spreadability studies are shown in **Table 3**. The TPA test suggested that the cohesiveness of the AmB-NE gel was sufficient, the work of adhesion was moderate, and the gel exhibited non-drip nature. The results of the spreadability test suggested that the AmB-NE gel is easily spreadable without

much work being done. The penetrometry test determined that the gel was soft enough for application.

3.5.3 *Ex-vivo* mucoadhesive test

Mucoadhesion can be measured in terms of the force or the work done. Still, the latter provides a better characterization of the detachment phenomenon, representing the sum of all the adhesive bonds established. As a result, the work done to detach the formulation from a tissue's surface was considered a better indicator of mucoadhesion. It can be noted from the values of the mucoadhesive test (**Table 3**) that the AmB-NE gel had sufficient mucoadhesive strength.

3.5.4 *Ex-vivo* retention measurement

Traditional vaginal drug delivery systems (VDDS) approaches are linked to limited retention, resulting in poor patient compliance due to the vaginal tract's self-cleaning activity. Mucoadhesive polymers are added to VDDS to solve this problem. By interacting with the vaginal mucosa, mucoadhesive polymers can keep drug delivery systems in the vaginal tube, increasing patient compliance and delivery system efficiency. The *ex-vivo* retention measurement demonstrated that the mucoadhesive gel base of the AmB-NE could hold the gel for 11 ± 0.4 h inside the vaginal cavity.

3.5.5 *In-vitro* drug release from the AmB-NE gel

After 12 hours, the percentage of AmB released from AmB-NE gel (84.33 ± 4.50%) was found to be significantly higher ($p<0.01$) than that of coarse AmB gel (66.80 ± 5.0%,) **(Fig. 4b).** The AmB-NE gel displayed a Higuchi model ($r^2=0.998$) among the various release models tested. The presence of a high r^2 value suggested a matrix diffusion-based mechanism for AmB release. When the *in-vitro* release data were fitted using the Korsmeyer-Peppas equation, the value of n ranged from 0.80 to 0.97, indicating a non-Fickian/anomalous diffusion release of AmB from the hydrophilic matrix.

3.5.6 *Ex-vivo* skin permeation studies

The *ex-vivo* skin penetration profile of the AmB-NE gel differed significantly from that of the coarse AmB gel (**Fig. 4c**). This was most likely due to the presence of solubilised AmB within the nanoemulsion droplets loaded in the gel. The steady-state flux (J_{ss}) and permeability coefficient (K_p) were found to be significantly enhanced ($p<0.01$). (Table 4). Furthermore, the enhancement ratio (E_r) revealed that AmB-NE gel improved AmB permeation by 4.26-fold

when compared to coarse AmB gel. In addition to the nano globule size of AmB-NE, solubilizers such as Capmul MCM, Cremophor RH 40, and permeation enhancer, Transcutol P, may have contributed to an increase in AmB-NE gel permeation into the mucosal layer.

3.5.7 Stability study of AmB-NE gel

Chemical stability experiments on AmB-NE gels at 5 ± 3 °C (**Table 5**) showed that the pH remained below 5 at all time periods and that there was no pH increase. It is therefore possible to draw the conclusion that the gel continued to be physiologically tolerable even after 180 days. The logarithm of percent drug remaining versus the time graph (days) (provided in supplementary data **Fig. S5**) indicated that 1.08% of AmB degraded in the AmB-NE gel after 180 days of storage.

3.5.8 *In vitro* antifungal activity

Using the cup plate method, the average zone of inhibition of AmB in DMSO against *Candida albicans* was found to be 22.60 ± 0.3 mm. In contrast, AmB-NE showed enhanced *in-vitro* antifungal activity, with an average zone of inhibition of 32.10 ± 0.4 mm. This could be attributed to the increased ability of nanosized AmB-containing oil globules to penetrate fungal cell walls. *Aloe vera* gel alone showed an average zone of inhibition of 37.10 ± 0.5 mm, whereas the average zone of inhibition increased tremendously ($p<0.05$) to 45.30 ± 0.5 mm in the case of the AmB-NE gel. This enhancement might have been a result of the combined effect of AmB-NE and *Aloe vera* gel. Furthermore, these findings suggested that AmB-NE gel was highly effective ($P<0.01$) against *Candida albicans* as compared to crude AmB.

3.6 In-vivo vaginal lavage testing

The HPLC analytical data showed that about 37.95 ± 4.5% of the drug was recovered in the vaginal lavage of the group treated with AmB-NE loaded gel, which indicates that 62.05 ± 8.6% of the AmB might have permeated the vaginal epithelium (**Fig. 5**). On the other hand, there was a recovery of 90.96 ± 4.0% in the group treated with coarse AmB gel, which indicates that only 8.82 ± 4% of the AmB permeated through the vaginal epithelium. As a result, the AmB-NE gel penetrated 7.03-fold higher than the coarse AmB gel. This could be due to nanoemulsion's ability to solubilize AmB into nanosized lipidic globules that penetrate the vaginal mucosal layer more efficiently than coarse AmB.

3.7 Histological study

A photomicrograph of the treated and untreated vaginal epithelium (**Fig. 6**) gives an idea of the damage that the formulation and its components can cause. Histology of untreated normal vaginal epithelium (control) and that of a damaged epithelium caused by treatment with isopropyl alcohol (IPA) is depicted in **Fig. 6a** and **6c**, respectively. It can be observed that AmB-NE (**Fig. 6b**), CA gel (**Fig. 6d**) and AmB-NE gel (**Fig. 6e**) did not display any detrimental effect on vaginal epithelium. The micrographs of test formulation treated rats showed that epithelial lining and lamina propria regions were intact.

4. Conclusions

The quest of the present study was to improve AmB's solubility and permeability in order to provide an alternative treatment against azole-resistant vulvovaginal candidiasis. Considering the said, a kinetically stable batch of AmB-NE formulation with a mean globule size of 76.52 ± 3.11 nm, PDI of 0.342 ± 0.032, and a zeta potential of -22.32 ± 0.88 m/V was formulated. This system was loaded into a Carbopol® 974P gel and *Aloe vera-based* gel-based system that facilitated its residence within the vaginal cavity for 11 ± 0.4 h. In addition, the prepared gel was found to be soft (0.21 ± 0.07 N) enough to ensure its spreadability (19.45 ± 0.5 g/s) into the vaginal cavity. According to the TPA specifications, the gel was sufficiently cohesive and firm to create a non-drip formulation that could sustain in the cavity. AmB-NE gel displayed a non-Fickian/anomalous release of AmB from the hydrophilic gel matrix. The pH of the formulated gel was 4.72 ± 0.30, which was consistent with the physiological pH of the vagina, and histopathologic studies confirmed its safety. In addition to AmB-NE gel's potential antifungal activity, *ex-vivo* permeation studies revealed that it could permeate 4.26-fold more than coarse-AmB gel. Similar results were obtained during in-vivo lavage experiments, wherein AmB-NE gel penetrated rat vaginal mucosa 7.03-fold more thoroughly than coarse-AmB gel. Thus, it is evident that, AmB's solubility increased after being transformed into a nanoemulsion, and that the nanosize of the droplets enabled its permeability into the vaginal mucosal layer. However, this research is still at the exploratory stage, and the question of scaling up needs to be resolved. Moreover, intensive studies and clinical trials are further required to realize the full potential of AmB-NE gel. Many problems in the research, production and application need to be resolved. From a future perspective, the authors believe that a more effective solubilizer, as well as an effective permeation enhancer, will be required to achieve a better formulation system. Hence, this investigation gives a ray of hope for developing a more promising formulation of AmB in a gel form for treating azole-resistant vulvovaginal candidiasis.

Conflict of interest

The authors report no conflicts of interest. The authors are responsible for the content and writing of the paper.

Funding statement

This work does not involve any funding source.

References

[1] Centers for Disease Control and Prevention. Vaginal Candidiasis. Natl Cent Emerg Zoonotic Infect Dis (NCEZID), Div Foodborne, Waterborne, Environ Dis 2022. https://www.cdc.gov/fungal/diseases/candidiasis/genital/index.html.

[2] Sobel JD, Faro S, Force RW, Foxman B, Ledger WJ, Nyirjesy PR, et al. Vulvovaginal candidiasis: Epidemiologic, diagnostic, and therapeutic considerations. Am J Obstet Gynecol 1998;178:203-211. https://doi.org/10.1016/S0002-9378(98)80001-X.

[3] Willems HME, Ahmed SS, Liu J, Xu Z, Peters BM. Vulvovaginal Candidiasis: A Current Understanding and Burning Questions. J Fungi 2020;6:27-31. https://doi.org/10.3390/jof6010027.

[4] Lima WG, Araújo MGF, Brito JCM, Castilho RO, Cardoso VN, Fernandes SOA. Antifungal effect of hydroethanolic extract of Fridericia chica (Bonpl.) L. G. Lohmann leaves and its therapeutic use in a vulvovaginal candidosis model. J Med Mycol 2022;32:101255. https://doi.org/10.1016/J.MYCMED.2022.101255.

[5] Schwebke JR, Sobel R, Gersten JK, Sussman SA, Lederman SN, Jacobs MA, et al. Ibrexafungerp Versus Placebo for Vulvovaginal Candidiasis Treatment: A Phase 3, Randomized, Controlled Superiority Trial. Clin Infect Dis 2022;74:1979-1985. https://doi.org/10.1093/cid/ciab750.

[6] Sobel JD, Nyirjesy P. Oteseconazole: An advance in treatment of recurrent vulvovaginal candidiasis. Future Microbiol 2021;16:390-411. https://doi.org/10.2217/fmb-2021-0173.

[7] Makanjuola O, Bongomin F, Fayemiwo SA. An update on the roles of non-albicans candida species in vulvovaginitis. J Fungi 2018;4:1-17. https://doi.org/10.3390/jof4040121.

[8] Nami S, Mohammadi R, Vakili M, Khezripour K, Mirzaei H, Morovati H. Fungal vaccines, mechanism of actions and immunology: A comprehensive review. Biomed Pharmacother 2019;109:333-354. https://doi.org/10.1016/j.biopha.2018.10.075.

[9] de Bastiani FWM da S, Spadari C de C, de Matos JKR, Salata GC, Lopes LB, Ishida K. Nanocarriers Provide Sustained Antifungal Activity for Amphotericin B and Miltefosine in the Topical Treatment of Murine Vaginal Candidiasis. Front Microbiol 2020;10:2976. https://doi.org/10.3389/fmicb.2019.02976.

[10] Johal HS, Garg T, Rath G, Goyal AK. Advanced topical drug delivery system for the management of vaginal candidiasis. Drug Deliv 2016;23:550-563. https://doi.org/10.3109/10717544.2014.928760.

[11] Lanchares JL, Hernández ML. Recurrent vaginal candidiasis changes in etiopathogenical patterns. Int J Gynecol Obstet 2000;71:29-35. https://doi.org/10.1016/s0020-7292(00)00352-0.

[12] Clemons K V., Sobel RA, Williams PL, Pappagianis D, Stevens DA. Efficacy of intravenous liposomal amphotericin B (AmBisome) against coccidioidal meningitis in rabbits. Antimicrob Agents Chemother 2002;46:2420-2436. https://doi.org/10.1128/AAC.46.8.2420-2426.2002.

[13] Grim SA, Smith KM, Romanelli F, Ofotokun I, Pérez A, Kaiser JM. Treatment of azole-resistant oropharyngeal candidiasis with topical amphotericin B. Ann Pharmacother 2002;36:1383-1396. https://doi.org/10.1345/aph.1C052.

[14] Hossain MA, Reyes GH, Long LA, Mukherjee PK, Ghannoum MA. Efficacy of caspofungin combined with amphotericin B against azole-resistant *Candida albicans*. J Antimicrob Chemother 2003;51:1427-1429. https://doi.org/10.1093/jac/dkg230.

[15] Patil M, Wanjare S, Borse V, Srivastava R, Mehta P, Vavia P. Arginolipid: A membrane-active antifungal agent and its synergistic potential to combat drug resistance in clinical Candida isolates. Arch Pharm (Weinheim) 2020;353:1-13. https://doi.org/10.1002/ardp.201900180.

[16] Neves J das, Amaral MH, Bahia MF. Performance of an *in vitro* mucoadhesion testing method for vaginal semisolids: Influence of different testing conditions and instrumental parameters. Eur J Pharm Biopharm 2008;69:622-632. https://doi.org/10.1016/j.ejpb.2007.12.007.

[17] Torrado JJ, Espada R, Ballesteros MP, Torrado-Santiago S. Amphotericin B formulations and drug targeting. J Pharm Sci 2008;97:2405–25. https://doi.org/10.1002/jps.21179.

[18] Adler-Moore J, Proffitt RT. AmBisome: Liposomal formulation, structure, mechanism of action and pre-clinical experience. J Antimicrob Chemother 2002;49:21-30. https://doi.org/10.1093/jac/49.suppl_1.21.

[19] Glavas-Dodov M, Fredro-Kumbaradzi E, Goracinova K, Simonoska M, Calis S, Trajkovic-Jolevska S, et al. The effects of lyophilization on the stability of liposomes containing 5-FU. Int. J. Pharm. 2005;291 79-86. https://doi.org/10.1016/j.ijpharm.2004.07.045.

[20] Anton N, Vandamme TF. Nano-emulsions and micro-emulsions: Clarifications of the critical differences. Pharm Res 2011;28:978–85. https://doi.org/10.1007/s11095-010-0309-1.

[21] Al-Subaie MM, Hosny KM, El-Say KM, Ahmed TA, Aljaeid BM. Utilization of nanotechnology to enhance percutaneous absorption of acyclovir in the treatment of herpes simplex viral infections. Int J Nanomedicine 2015;10:3973-3985. https://doi.org/10.2147/IJN.S83962.

[22] Shahid M, Hussain A, Khan AA, Alanazi AM, Alaofi AL, Alam M, et al. Antifungal

Cationic Nanoemulsion Ferrying Miconazole Nitrate with Synergism to Control Fungal Infections: *In Vitro*, *Ex Vivo*, and *In Vivo* Evaluations. ACS Omega 2022;7:13343–53. https://doi.org/10.1021/acsomega.2c01075.

[23] Kumar S, Ali J, Baboota S. Design Expert® supported optimization and predictive analysis of selegiline nanoemulsion via the olfactory region with enhanced behavioural performance in Parkinson's disease. Nanotechnology 2016;27:435101. https://doi.org/10.1088/0957-4484/27/43/435101.

[24] Hardy E, De Pádua KS, Jiménez AL, Zaneveld LJD. Women's preferences for vaginal antimicrobial contraceptives I: Methodology. Contraception 1998;58:245-249. https://doi.org/10.1016/S0010-7824(98)00105-X.

[25] Dal'Belo SE, Rigo Gaspar L, Maia Campos PMBG. Moisturizing effect of cosmetic formulations containing *Aloe vera* extract in different concentrations assessed by skin bioengineering techniques. Ski Res Technol 2006;12:241-246. https://doi.org/10.1111/j.0909-752X.2006.00155.x.

[26] Fani M, Kohanteb J. Inhibitory activity of *Aloe vera* gel on some clinically isolated cariogenic and periodontopathic bacteria. J Oral Sci 2012;54:15-21. https://doi.org/10.2334/josnusd.54.15.

[27] Davis RH, Leitner MG, Russo JM, Byrne ME. Anti-inflammatory activity of *Aloe vera* against a spectrum of irritants. J Am Podiatr Med Assoc 1989;79:263-276. https://doi.org/10.7547/87507315-79-6-263.

[28] Hamman JH. Composition and applications of *Aloe vera* leaf gel. Molecules 2008;13:1599-1616. https://doi.org/10.3390/molecules13081599.

[29] Vázquez B, Avila G, Segura D, Escalante B. Antiinflammatory activity of extracts from Aloe vera gel. J Ethnopharmacol 1996;55:69-75. https://doi.org/10.1016/S0378-8741(96)01476-6.

[30] Mohsin AH Bin, Varalakshmi Reddy S, Praveen Kumar M, Samee S. *Aloe vera* for dry mouth denture patients – Palliative therapy. J Clin Diagnostic Res 2017;11:ZC20-ZC23. https://doi.org/10.7860/JCDR/2017/25084.10036.

[31] Shafiq S, Shakeel F, Talegaonkar S, Ahmad FJ, Khar RK, Ali M. Development and bioavailability assessment of ramipril nanoemulsion formulation. Eur J Pharm Biopharm 2007;66:227-343. https://doi.org/10.1016/j.ejpb.2006.10.014.

[32] Xi J, Chang Q, Chan CK, Meng ZY, Wang GN, Sun JB, et al. Formulation development and bioavailability evaluation of a self-nanoemulsified drug delivery system of oleanolic acid. AAPS PharmSciTech 2009;10:172–82. https://doi.org/10.1208/s12249-009-9190-9.

[33] Tenjarla S. Microemulsions: An overview and pharmaceutical applications. Crit Rev Ther Drug Carrier Syst 1999;16:111-125. https://doi.org/10.1615/critrevtherdrugcarriersyst.v16.i5.20.

[34] Kreilgaard M, Pedersen EJ, Jaroszewski JW. NMR characterisation and transdermal drug delivery potential of microemulsion systems. J Control Release 2000;69:421-433. https://doi.org/10.1016/S0168-3659(00)00325-4.

[35] Anton N, Vandamme TF. Anton, N. & Vandamme, T.F. The universality of low-energy nano-emulsification. Int J Pharm 2009;377:978-985. https://doi.org/10.1016/j.ijpharm.2009.05.014

[36] Teo BSX, Basri M, Zakaria MRS, Salleh AB, Rahman RNZRA, Rahman MBA. A potential tocopherol acetate loaded palm oil esters-in-water nanoemulsions for nanocosmeceuticals. J Nanobiotechnology 2010;8:1-11. https://doi.org/10.1186/1477-3155-8-4.

[37] Chalikwar SS, Mene BS, Pardeshi C V., Belgamwar VS, Surana SJ. Self-Assembled, Chitosan Grafted PLGA Nanoparticles for Intranasal Delivery: Design, Development and Ex Vivo Characterization. Polym - Plast Technol Eng 2013;52:368-380. https://doi.org/10.1080/03602559.2012.751999.

[38] Chalikwar SS, Belgamwar VS, Talele VR, Surana SJ, Patil MU. Formulation and evaluation of Nimodipine-loaded solid lipid nanoparticles delivered via lymphatic transport system. Colloids Surfaces B Biointerfaces 2012;97:109-116. https://doi.org/10.1016/j.colsurfb.2012.04.027.

[39] Yilmaz E, Borchert HH. Design of a phytosphingosine-containing, positively-charged nanoemulsion as a colloidal carrier system for dermal application of ceramides. Eur J Pharm Biopharm 2005;60:91-98. https://doi.org/10.1016/j.ejpb.2004.11.009.

[40] Sonneville-Aubrun O, Simonnet JT, L'Alloret F. Nanoemulsions: A new vehicle for skincare products. Adv Colloid Interface Sci 2004;108:145-149. https://doi.org/10.1016/j.cis.2003.10.026.

[41] Parveen R, Baboota S, Ali J, Ahuja A, Vasudev SS, Ahmad S. Oil based nanocarrier for improved oral delivery of silymarin: *In vitro* and *in vivo* studies. Int J Pharm 2011;413:245–53. https://doi.org/10.1016/j.ijpharm.2011.04.041.

[42] Kelmann RG, Kuminek G, Teixeira HF, Koester LS. Determination of carbamazepine in parenteral nanoemulsions: Development and validation of an HPLC method. Chromatographia 2007;66:231-239. https://doi.org/10.1365/s10337-007-0314-7.

[43] Kumar M, Misra A, Babbar AK, Mishra AK, Mishra P, Pathak K. Intranasal nanoemulsion based brain targeting drug delivery system of risperidone. Int J Pharm 2008;358:285-291. https://doi.org/10.1016/j.ijpharm.2008.03.029.

[44] Echevarría I, Barturen C, Renedo MJ, Dios-Viéitez MC. High-performance liquid chromatographic determination of amphotericin B in plasma and tissue. Application to pharmacokinetic and tissue distribution studies in rats. J. Chromatogr. A.1998,819:156-159 https://doi.org/10.1016/S0021-9673(98)00425-7.

[45] Bilensoy E, Çırpanlı Y, Şen M, Doğan AL, Çalış S. Thermosensitive mucoadhesive gel formulation loaded with 5-Fu: Cyclodextrin complex for HPV-induced cervical cancer. J. Incl. Phenom. Macrocycl. Chem., vol. 57, 2007, p. 363-370. https://doi.org/10.1007/s10847-006-9259-y.

[46] Singh KK, Vingkar SK. Formulation, antimalarial activity and biodistribution of oral lipid nanoemulsion of primaquine. Int J Pharm 2008;347:136-143. https://doi.org/10.1016/j.ijpharm.2007.06.035.

[47] Bali V, Ali M, Ali J. Study of surfactant combinations and development of a novel

nanoemulsion for minimising variations in bioavailability of ezetimibe. Colloids Surfaces B Biointerfaces 2010;76:410-420. https://doi.org/10.1016/j.colsurfb.2009.11.021.

[48] Kim JY, Yi BR, Lee C, Gim SY, Kim MJ, Lee JH. Effects of pH on the rates of lipid oxidation in oil-water system. Appl Biol Chem 2016;59:157-167. https://doi.org/10.1007/s13765-015-0146-3.

[49] Klang V, Matsko N, Raupach K, El-Hagin N, Valenta C. Development of sucrose stearate-based nanoemulsions and optimisation through γ-cyclodextrin. Eur J Pharm Biopharm 2011;79:58-67. https://doi.org/10.1016/j.ejpb.2011.01.010.

[50] Bachhav YG, Patravale VB. Microemulsion based vaginal gel of fluconazole: Formulation, *in vitro* and *in vivo* evaluation. Int J Pharm 2009;365:175-179. https://doi.org/10.1016/j.ijpharm.2008.08.021.

[51] Bhowmik BB, Nayak BS, Chatterjee A. Formulation development and characterization of metronidazole microencapsulated bioadhesive vaginal gel. Int J Pharm Pharm Sci 2009;9:240-257.

[52] das Neves J, Pinto E, Teixeira B, Dias G, Rocha P, Cunha T, et al. Local Treatment of Vulvovaginal Candidosis. Drugs 2008;68:1787-1802. https://doi.org/10.2165/00003495-200868130-00002.

[53] Patel A, Patel J. Mucoadhesive Microemulsion Based Prolonged Release Vaginal Gel for Anti-Fungal Drug. Am J PharmTech Res 2012;2:650-661.

[54] Tasdighi E, Azar ZJ, Mortazavi SA. Development and *In-vitro* evaluation of a contraceptive vagino-adhesive propranolol hydrochloride gel. Iran J Pharm Res 2012;11:13–26.

[55] Bachhav YG, Patravale VB. Microemulsion-based vaginal gel of clotrimazole: formulation, *in vitro* evaluation, and stability studies. AAPS PharmSciTech 2009;10:476–81. https://doi.org/10.1208/s12249-009-9233-2.

[56] Ahmad FJ, Alam MA, Khan ZI, Khar RK, Ali M. Development and *in vitro* evaluation of an acid buffering bioadhesive vaginal gel for mixed vaginal infections. Acta Pharm 2008;58:407-419. https://doi.org/10.2478/v10007-008-0023-2.

[57] Belgamwar VS, Patel HS, Joshi AS, Agrawal A, Surana SJ, Tekade AR. Design and development of nasal mucoadhesive microspheres containing tramadol HCl for CNS targeting. Drug Deliv 2011;18:353-360. https://doi.org/10.3109/10717544.2011.557787.

[58] Satturwar PM, Fulzele S V., Dorle AK. Evaluation of polymerized rosin for the formulation and development of transdermal drug delivery system: A technical note. AAPS PharmSciTech 2005;6:E649–E654. https://doi.org/10.1208/pt060481.

[59] Barditch-Crovo P, Witter F, Hamzeh F, McPherson J, Stratton P, Alexander NJ, et al. Quantitation of vaginally administered nonoxynol-9 in premenopausal women. Contraception 1997;55:261-263. https://doi.org/10.1016/S0010-7824(97)00003-6.

[60] Reddy KVR, Aranha C, Gupta SM, Yedery RD. Evaluation of antimicrobial peptide nisin as a safe vaginal contraceptive agent in rabbits: *In vitro* and *in vivo* studies.

Reproduction 2004;128:117-126. https://doi.org/10.1530/rep.1.00028.

[61] Azeem A, Rizwan M, Ahmad FJ, Iqbal Z, Khar RK, Aqil M, et al. Nanoemulsion components screening and selection: A technical note. AAPS PharmSciTech 2009;10:96-76. https://doi.org/10.1208/s12249-008-9178-x.

[62] Craig DQM, Barker SA, Banning D, Booth SW. An investigation into the mechanisms of self-emulsification using particle size analysis and low frequency dielectric spectroscopy. Int J Pharm 1995;114:103-110. https://doi.org/10.1016/0378-5173(94)00222-Q.

Table 1a. Stress testing of formulation batches of AmB-NE (n=3, SD)

Batch code	Oil (% w/w)	S_{mix} (2:1 % w/w)	Water (% w/w)	Effect on mean globule size (nm) after stress testing				Inference
				Dilution test			Temp (45 °C, 48 h)	
				no dilution	10 times	100 times		
F1	24	24	52	114.98 ± 2.8	78.87 ± 3.2	67.68 ± 3.2	134.98 ± 3.2	Failed
F2	28	24	48	123.43 ± 3.4	89.45 ± 3.2	83.09 ± 2.6	Cracking	Failed
F3	32	24	44	137.67 ± 2.4	97.90 ± 2.2	56.90 ± 4.5	Cracking	Failed
F4	24	30	46	97.64 ± 2.2	66.78 ± 2.4	45.22 ± 2.4	113.21 ± 1.5	Failed
F5	28	30	42	99.94 ± 2.4	45.98 ± 2.4	43.98 ± 2.5	121.40 ± 3.2	Failed
F6	32	30	38	102.65 ± 2.4	77.98 ± 3.0	65.80 ± 2.5	Cracking	Failed
F7	**24**	**36**	**40**	**76.52 ± 3.11**	**76.32 ± 2.0**	**76.04 ± 3.4**	**78.65 ± 2.0**	**Passed**
F8	28	36	36	79.67 ± 1.5	65.96 ± 3.2	55.08 ± 2.4	108.23 ± 3.2	Failed
F9	32	36	32	80.88 ± 2.5	67.90 ± 4.2	34.89 ± 3.4	123.98 ± 3.0	Failed
F10	**24**	**42**	**34**	**71.60 ± 4.6**	**71. 80 ± 3.2**	**72.54 ± 4.4**	**72.21 ± 3.4**	**Passed**
F11	**28**	**42**	**30**	**81.96 ± 7.2**	**82.28 ± 3.5**	**83.11 ± 4.6**	**83.23 ± 1.5**	**Passed**

***** Bold section represents the results of formulations that passed the stress test.

Table 1b. Mean globule size, PDI, zeta potential, and rate of Ostwald ripening of AmB-NE formulations that passed the stress test (mean ± SD, n = 3)

Formulation	Globule size (nm)	PDI	Zeta potential (mV)	Rate of Ostwald ripening (x^3) (nm/day)
F7	**76.52 ± 3.11**	**0.342 ± 0.032**	**-22.32 ± 0.88**	**438.1 ± 7.59**
F10	71.60 ± 4.6	0.395 ± 0.045	-22.11 ± 0.20	986.3 ± 6.45
F11	81.96 ± 7.2	0.407 ± 0.034	-23.46 ± 0.20	1369.0 ± 9.32

*x^3 denotes values listed in the column of the rate of Ostwald ripening. The bold section represents the results of the optimised formulation.

Table 2. Stability of AmB-NE at 5 ± 3°C and 25 ± 2 °C, 60 ± 5% RH (mean ± SD, n = 3)

Condition	Time (days)	Globule size (nm)	PDI	Zeta potential (mV)	pH	Viscosity (cP)	% AmB remaining	Log_{10} AmB remaining
5 ± 3 °C	0	76.52 ± 3.11	0.342 ± 0.03	-22.32 ±0.88	6.83 ± 0.47	86.22 ±1.41	100.0	2.000
	60	76.66 ± 7.77	0.361 ± 0.03	-22.39 ±0.44	6.88 ± 0.43	86.32 ±1.55	99.56	1.998
	120	77.32 ± 7.98	0.389 ± 0.07	-22.65 ±0.67	6.93 ± 0.4	86.33 ±0.93	99.12	1.996
	180	77.98 ± 8.23	0.401 ± 0.02	-22.77 ±0.95	7.32 ± 0.45	86.37 ±1.21	98.35	1.991
25 ± 2 °C	0	76.52 ± 3.11	0.342 ± 0.03	-22.32 ±0.88	6.83 ± 0.47	86.22 ±1.41	100.0	2.000
	60	78.97 ± 4.87	0.386 ± 0.04	-22.11± 0.78	6.91 ± 0.7	86.56 ±1.95	87.25	1.940
	120	86.54 ± 5.20	0.487 ± 0.14	-21.98± 0.32	6.43 ± 0.65	86.68 ±1.50	76.98	1.886
	180	97.90 ± 6.08	0.492 ± 0.18	-22.67± 0.64	6.78 ± 0.66	86.93 ±1.65	66.78	1.824

*Stability studies of AmB-NE were performed in a sealed amber-coloured glass vial

Table 3. Results of texture profile analysis (TPA), spreadability, penetrometry, and mucoadhesive test conducted on AmB-NE gel (mean ± SD, n = 3)

Sr. No.	Test	Values
1.	**TPA parameters**	
	a. Hardness/firmness (g)	36.70 ± 2.0
	b. Work of adhesion (g.s)	20.84 ± 3.20
	c. Cohesiveness	0.54 ± 0.2
	d. Springiness (mm)	28.36 ± 0.82
2.	**Spreadability (g/s)**	19.45 ± 0.5
3.	**Penetrometry (N)**	0.21 ± 0.07
4.	**Mucoadhesive test**	
	a. Work done (mJ)	1.75 ± 0.40
	b. Force (N)	0.47± 0.15

*TPA test revealed mechanical (sensory) properties of AmB-NE gel whereas spreadability and penetrometry gave an idea of ease of application and softness of the gel.

Table 4. Permeability parameters of AmB-NE gel and coarse AmB gel (mean ± SD, n = 3)

Formulation	**J_{ss}(μg/cm^2/h)**	**K_p (cm/h) ×10^{-3}**	**E_r**
Coarse AmB gel	7.38 ± 2.021	2.46 ± 0.091	-----
AmB-NE gel	31.45 ± 3.430	10.49 ± 0.141	4.26

*J_{ss} and K_p represent steady-state flux and permeability coefficient of tested gels respectively. E_r represents the enhancement ratio of AmB-NE gel when compared to coarse AmB gel

Table 5. Stability study of AmB-NE gel at 5 ± 3°C (mean ± SD, *n* = 3)

Time (days)	pH	% drug remained	Log_{10} drug remained
0	4.72 ± 0.32	100.0	2.0000
60	4.77 ± 0.24	99.85	1.9993
120	4.81 ± 0.90	99.34	1.9971
180	4.86 ± 0.78	98.92	1.9952

*AmB-NE gel was stored in aluminium tubes

a

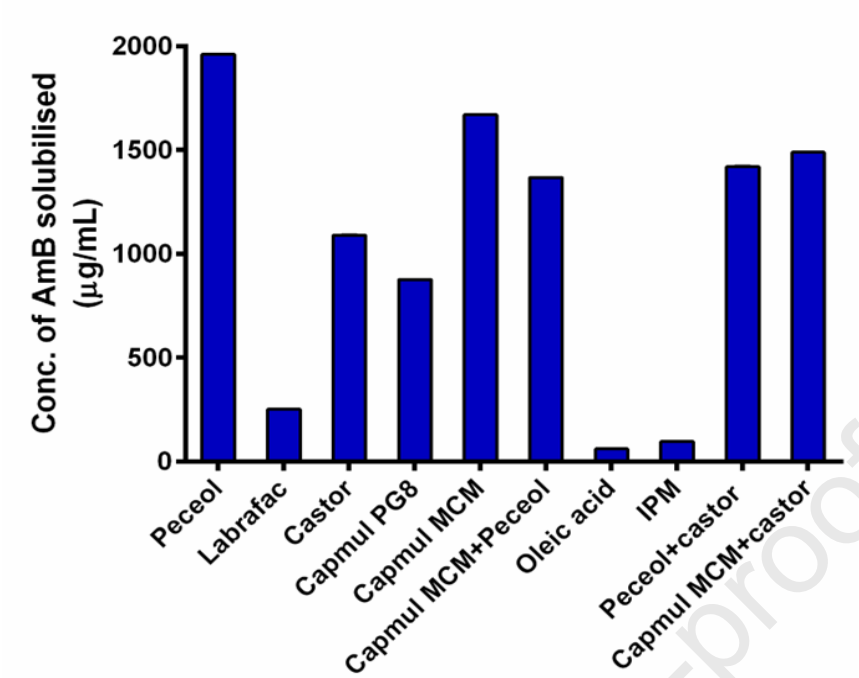

b

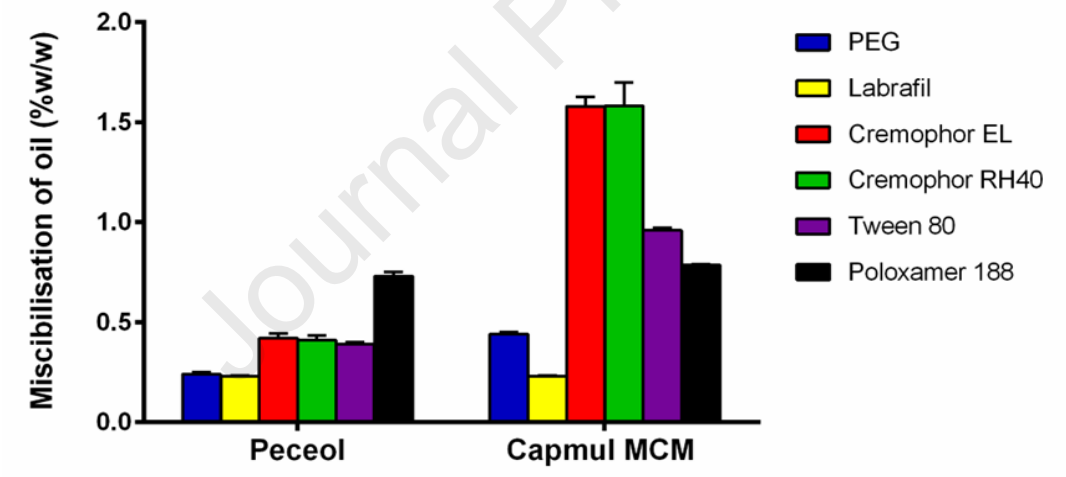

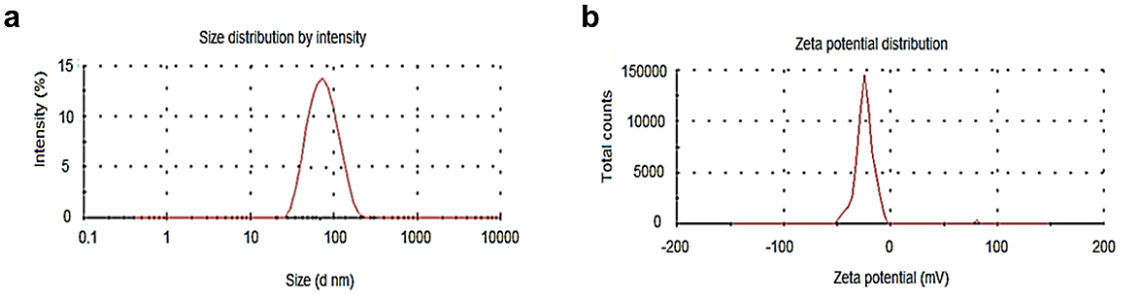

Figure 2: a. Globule size (nm) and **b.** Zeta potential (mV) of AmB-NE obtained by zetasizer instrument operated at 25 °C

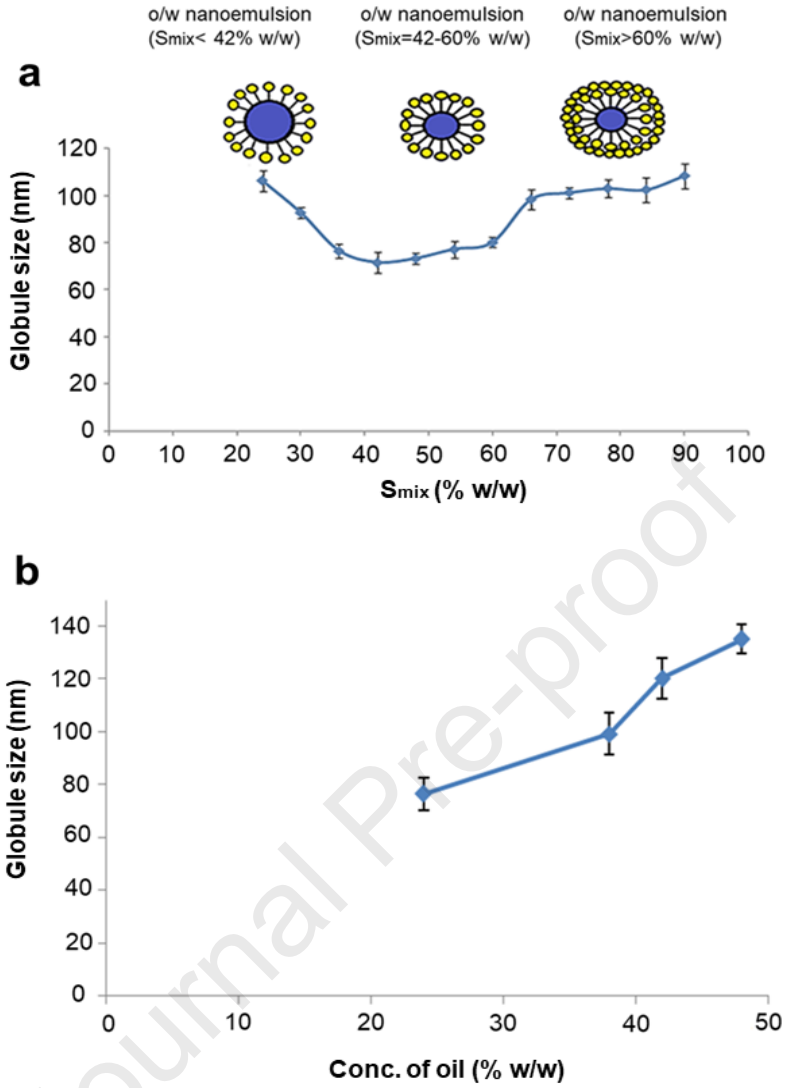

Figure 3: The graphical plot represents **a.** changes in AmB-NE's mean globule after subjecting it to variable S_{mix} concentration (24-90% w/w) while having a constant concentration of oil phase (24% w/w). **b**. represents changes in mean globule size of AmB-NE after subjecting it to variable oil (Capmul MCM) concentration (24-90% w/w) while having a constant concentration of S_{mix} phase (24-48% w/w).

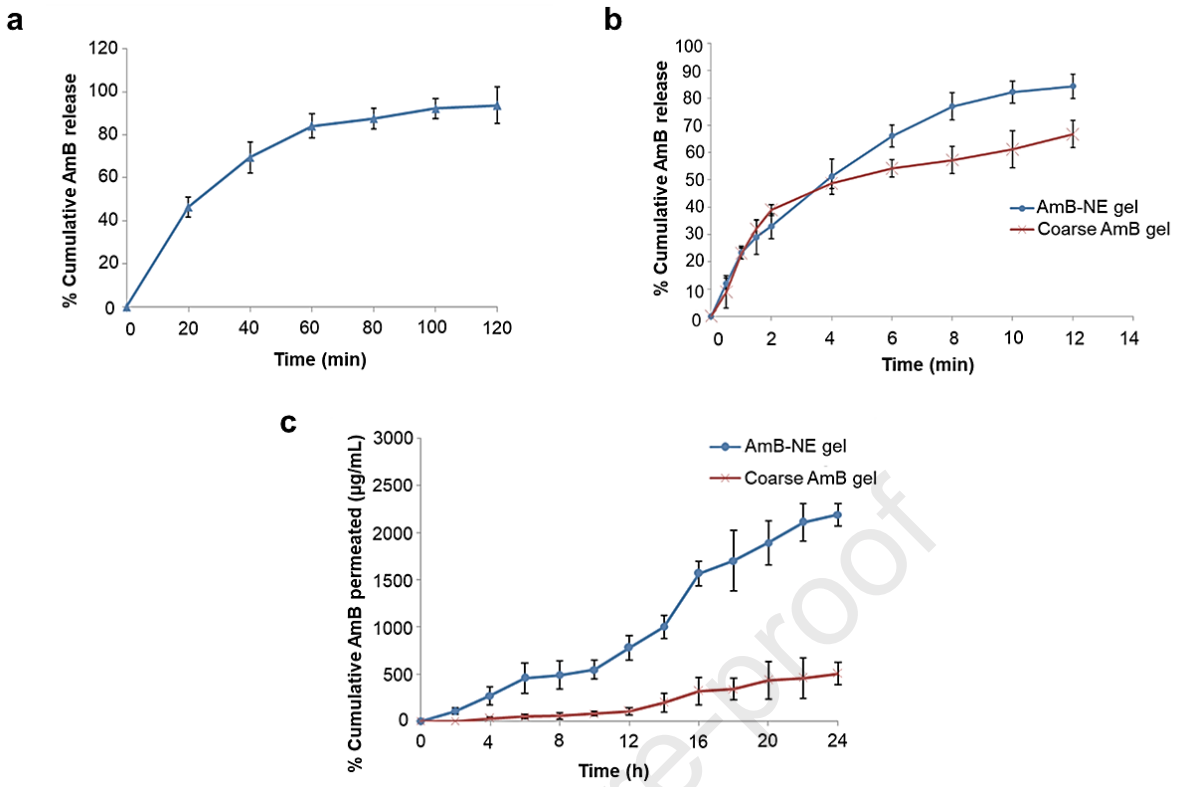

Figure 4: Graphical representation of **a.** *In-vitro* drug release profile of AmB-NE performed in 50 mL of citro-phosphate buffer (pH 4.5) containing DMSO and methanol (1:1). **b.** *In-vitro* drug release profile of AmB-NE gel (blue) and coarse AmB gel (red) performed in 500 mL of citro-phosphate buffer (pH 4.5) containing 2% of DMSO and methanol (1:1). **c.** *Ex-vivo* skin permeation of AmB-NE gel (blue) and coarse AmB gel (red) across bovine vaginal mucosa performed in citro-phosphate buffer (pH 4.5) complemented with 2% of DMSO and methanol (1:1) using a Franz diffusion cell.

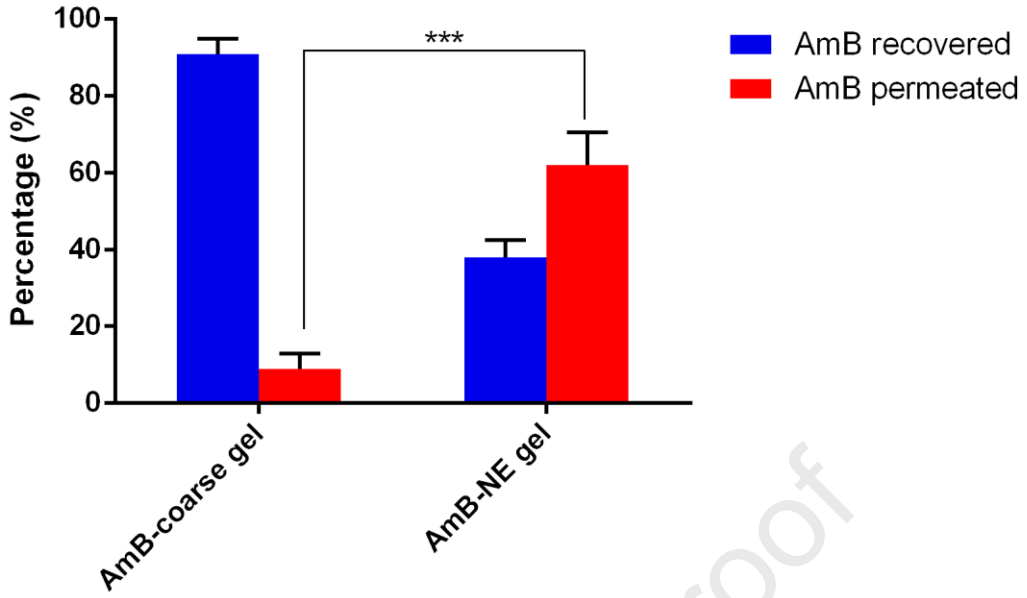

Figure 5: Bar graph representing *in-vivo* vaginal lavage studies performed in female Sprague Dawley rats. The bar graph compares the percent AmB recovered in vaginal lavage samples taken after 24 h of application (blue) along with the estimated % AmB permeated through the vaginal mucosal layer (red). *** represents the $p<0.001$.

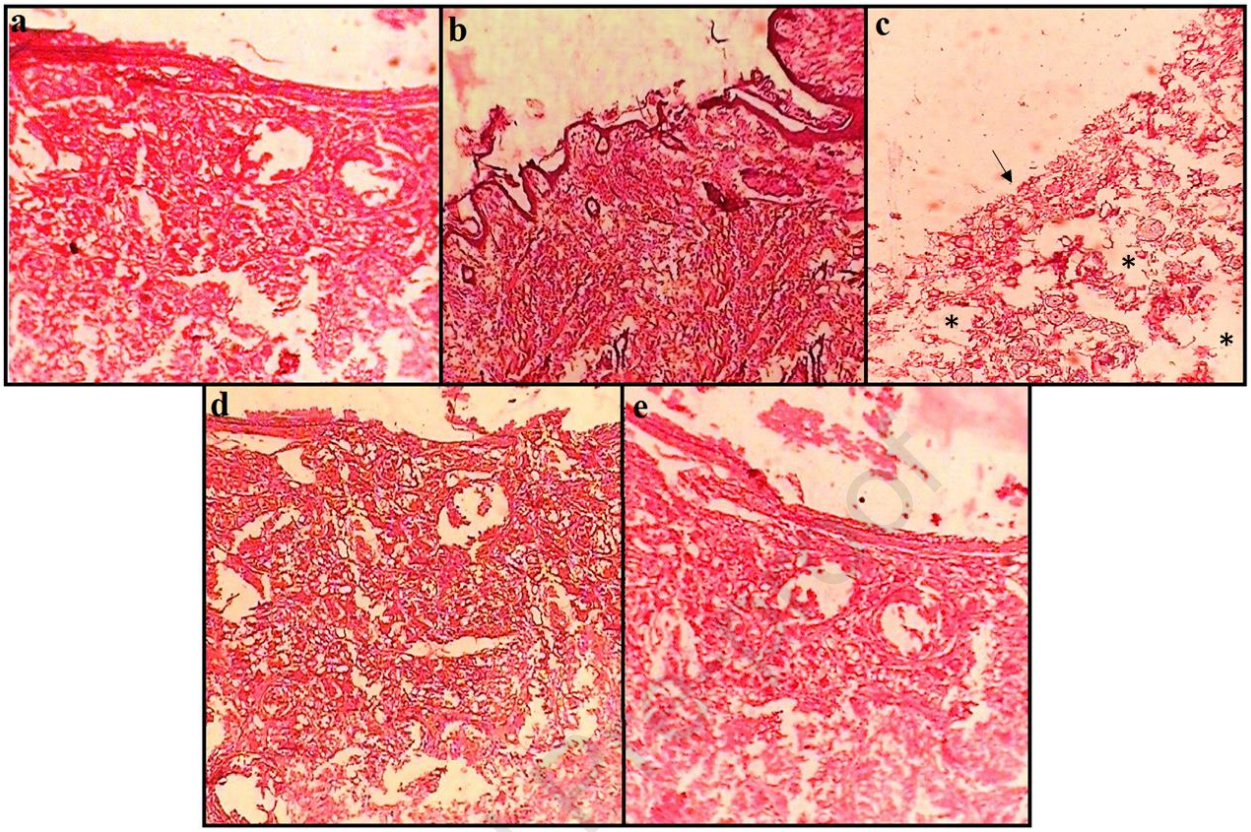

Figure 6: Histological micrographs of Sprague Dawley rat vaginal epithelium stained with haematoxylin and eosin showing the following treatments: **a.** saline (control), **b.** AmB-NE, **c.** isopropyl alcohol, **d.** Carbopol® 974P and *aloe vera* gel (CA gel), and **e.** AmB-NE gel. Figure 6c depicts a disrupted and non-continuous (broken) stratum epithelium, with stars (*) indicating damaged lamina propria regions.